ELECTROMAGNETIC CHARACTERIZATION OF THE FIRST IPHI RFQ SECTION

François SIMOENS†, Alain FRANCE, Jacques GAIFFIER,
CEA SACLAY, 91191 Gif-sur-Yvette, FRANCE

Abstract

During the process of manufacturing the High Intensity Proton Injector project (IPHI) RFQ, electromagnetic measurements are to be applied to each single 1 meter long Copper segment before and after brazing. These RF tests evaluate the longitudinal distribution of the mechanical disequilibria and constitute the unique diagnostics after brazing. Conditions and results of the characterization of the first RFQ section are presented.

1 INTRODUCTION

A new RF diagnostic extracts the mechanical defaults of the central region delimited by the vanes tips from the bead-pull field measurement. Experimental tests on our RFQ cold-model have validated this method [1]. The electromagnetic characteristics of the first IPHI RFQ section have been estimated to answer 2 questions:

1- Has the brazing procedure modified the transverse section equilibrium ?
2- Is this first section tunable ?

2 MEASUREMENT BENCH

For bead-pull field measurements [2], a pulley system guiding the wire successively through the 4 quadrants stays permanently in the factory site (Fig. 1). The rest of the equipment is carried in situ for each RF test.

2.1 Guiding position in the transverse section

Three possible positions of the bead trajectory in the transverse section have been specifically studied in the transverse section on our cold-model:

1- The variation of the IPHI RFQ cross section forbids the guiding of a dielectric object leaning on the vane tips in the electric field region (Pos #1 in Fig. 2).

2 & 3- The *H* magnetic field perturbation has been tested in the outer quadrant by the tuner side (Pos #2) and on the bisector (Pos #3).

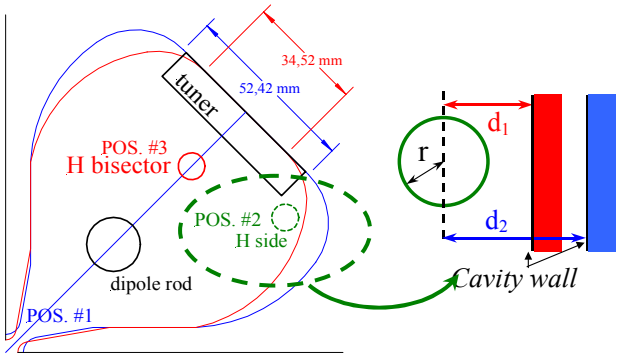

Fig. 2: variation of the IPHI RFQ cross-section

On the location #3, because of the cross section evolution, the distance *d* between the center of a metallic bead and the nearest wall varies approximately from d_1=*8 mm* to d_2=*17 mm* (Fig. 2). J. Gao [3] expresses the field induced by charges on planar cavity wall that has to be added to the measured field perturbed by a spherical bead. The consequent extra frequency shift $\Delta f(r,d)$ of this image effect is a function of the bead radius *r* and of *d*.

	r=4 mm	*r=6 mm*
$[\ \Delta f(r,d_1)/\ \Delta f(r,\infty)\ ] - 1$	-1.8 %	-8.5 %
$[\ \Delta f(r,d_2)/\ \Delta f(r,\infty)\ ] - 1$	-0.2 %	-0.9 %

When *r=4 mm*, the combination of cross section evolution and image effect generates a 1.6 percent variation of the measured field. It dramatically increases with the radius. Compared to the 4 mm radius olive-like metallic bead that we normally use, this effect is not negligible on the path close to the tuner side. That is not the case at the bisector location that is farther from the moving walls ($d \approx 30$ *mm*). The image effect cannot be easily compensated since the bead is not a sphere, and moreover the cavity walls are not planar. This phenomenon has led to the choice of a measurement on the bisector.

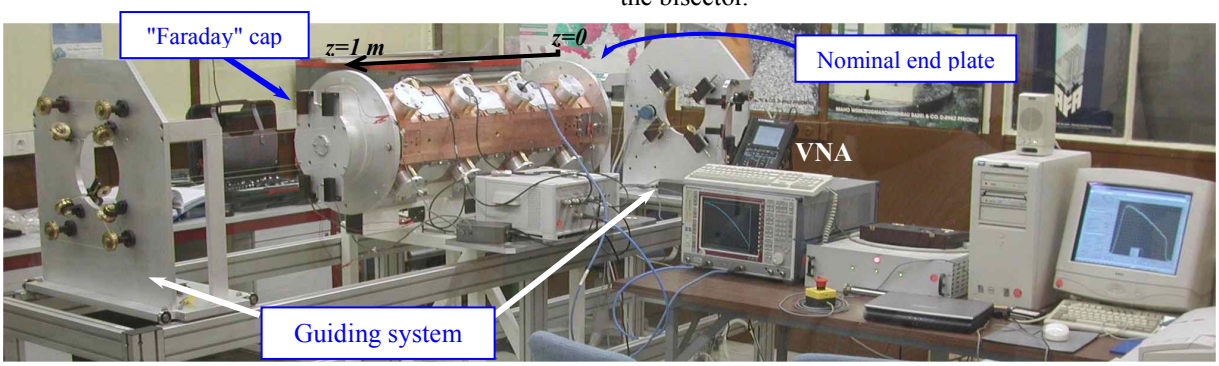

Fig. 1: bead-pull field measurement bench characterizing the first IPHI RFQ section on the factory site

†fsimoens@cea.fr

2.2 Three tests series

Three RF tests have been made:

- RF1: Before brazing and before finishing machinings.
- RF2: Before brazing and **after** finishing machinings.
- RF3: After brazing

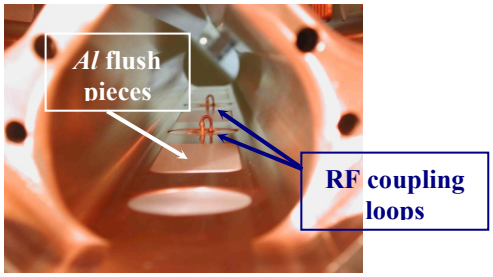

Fig. 3: inside view of 1 quadrant (RF1)

During RF1 tests, the pumping ports of the first section were initially closed by aluminum flush pieces (Fig. 3). Measurements have been made adding one and then 3 pumping grids in a single quadrant.

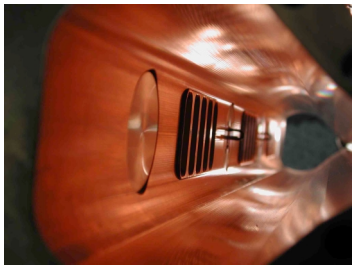

Fig. 4: inside view of one quadrant with pumping grids

The RFQ section was completely equipped during RF2 and RF3 tests (Fig. 4).

3 FREQUENCY & Q EVOLUTION

The pumping grids depth inside the cavity is designed to compensate for the frequency shift induced by the openings [4]. Actually, the addition of pumping grids causes a small decrease -roughly 20 kHz / pumping grids port - of the quadrupole resonance frequency (Table 1).

Table 1: Measured parameters

	f_0	Δf_D	Q
RF1 (no pumping grid)	352,496 MHz	270 kHz	2800
RF1 (1 pumping grid)	352,478 MHz	271 kHz	
RF1 (3 pumping grids)	352,451 MHz	279 kHz	
RF2 equipped	352,885 MHz	500 kHz	4636
RF3 equipped	353,002 MHz	402 kHz	6752

A relevant criterion of the transverse equilibrium evolution is the frequency difference Δf_D between the 2 dipolar resonances (Fig. 4). In a perfectly symmetrical RFQ, $\Delta f_D=0$. The 3 configurations of RF1 show a negligible effect of the added pumping grids (Table 1). The finishing machining step has slightly deteriorated the equilibrium that was almost recovered after brazing (RF3).

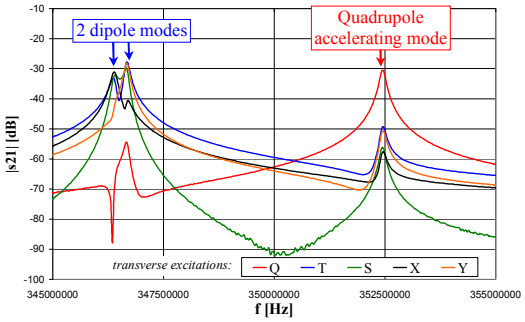

Fig. 4: 1st dipole and quadrupole modes (before brazing)

The replacement of the dummy flush Al pieces by the OFCE copper grids has almost doubled the quality factor (Q). The Q of the brazed section is equal to 65% of the theoretical 2d value though temporary aluminium pieces are closing the end regions. It traduces a high quality of the surface and better RF contacts.

4 MODAL COMPONENTS OF THE ACCELERATING VOLTAGE

The abruptly cut end represents a strong detuning of the boundary conditions. The quadrupole component $uQ(z)$ of the accelerating voltage slopes down deeply (Fig. 5). The small decrease of the slope from one RF test to the next. is mainly due the mechanical modifications of the end regions at each step.

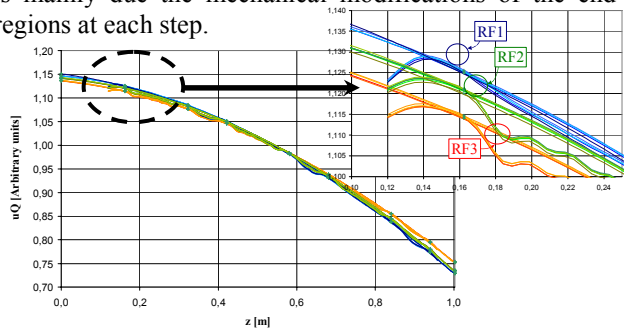

Fig. 5: $uQ(z)$ evolution

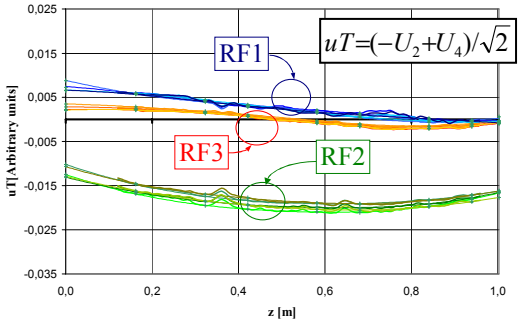

Fig. 6: $uT(z)$ evolution

The best equilibrium is diagnosed at RF1 where the dipole components $|uS(z)|$ & $|uT(z)| < 5.10^{-3}$ compared to a unitary mean $|uQ(z)|$. The RF2 tests show a increase of the mean $|uS(z)|$ $(\approx 4.10^{-2})$ & $|uT(z)|$ $(\approx 2.10^{-2})$. The brazing (RF3) has corrected the T dipolar unbalance but left the S

orientation unchanged. This modal component estimation is coherent with the "Δf_D" diagnostic.

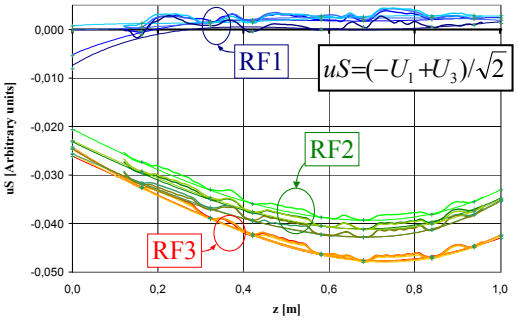

Fig. 7: *uS(z)* evolution

5 CAPACITANCES ESTIMATION

Table 2: capacitances and distances equivalences

$dC_{QQ}=1/4\sum_{k=1}^{4} dC_k$	$\propto$	$-\sum_{k=1}^{4}\left(\frac{d_k^m-d_k^r}{d_k^r}\right)$
$dC_{SQ}/C=[1/2[dC_1-dC_3]/C]-1$	$\propto$	$\left(\frac{d_1^m-d_1^r}{d_1^r}\right)-\left(\frac{d_3^m-d_3^r}{d_3^r}\right)$
$dC_{TQ}/C=[1/2[dC_4-dC_2]/C]-1$	$\propto$	$-\left(\frac{d_4^m-d_4^r}{d_4^r}\right)+\left(\frac{d_2^m-d_2^r}{d_2^r}\right)$

The capacitances defaults are related to the relative errors of the corresponding combined mechanical distances d_i between neighbouring electrodes (Table 2 where *"k"* denotes the quadrant number; *"m"* measured, *"r"* reference. The d_k have been measured by a 3d mechanical probe at each RFQ section end

Table 3: relative errors evolutions

	End z=0 m		*End z=1 m*	
	$\delta(d_4, d_2)$	dC_{TQ}/C	$\delta(d_4, d_2)$	dC_{TQ}/C
RF1	**$0{,}22.10^{-3}$**	**$\approx+0{,}3.10^{-3}$**	**$-0{,}35.10^{-3}$**	**$\approx-0.2.10^{-3}$**
RF2	$0{,}40.10^{-3}$	$\approx+0{,}1.10^{-3}$	$-1.42.10^{-3}$	$\approx+0.4.10^{-3}$
RF3	**$0.22.10^{-3}$**	**$\approx+0{,}3.10^{-3}$**	**$-0.92.10^{-3}$**	**$\approx-0.9.10^{-3}$**

	End z=0 m		*End z=1 m*	
	$\delta(d_1, d_3)$	dC_{SQ}/C	$\delta(d_1, d_3)$	dC_{SQ}/C
RF1	**$-0{,}47.10^{-3}$**	**$\approx-0{,}2.10^{-3}$**	**$-0{,}30.10^{-3}$**	**$\approx0.10^{-3}$**
RF2	$+0{,}95.10^{-3}$	$\approx1{,}8.10^{-3}$	$-1{,}47.10^{-3}$	$\approx-0{,}8.10^{-3}$
RF3	**$+2{,}12.10^{-3}$**	**$\approx+1{,}8.10^{-3}$**	**$0{,}73.10^{-3}$**	**$\approx0{,}7.10^{-3}$**

An excellent correspondence is observed between the mechanical data and dC_{SQ} and dC_{TQ} estimated in RF1 and RF3 (the mean value of 4 measurements per test is considered). The RF2 tests are unfortunately not reliable because measured fields suffer from bad wire alignment and unstable mechanical support of the RFQ section.

The sign (dC_1/C α $-\delta d/d^r$) and the order of magnitude agree, and all the more for higher defaults (Table 3). So the mechanical defaults profiles can be reliably estimated from RF1 and RF3 electromagnetic diagnostics.

The brazing has not modified the small T dipole unbalance (Fig. 8).

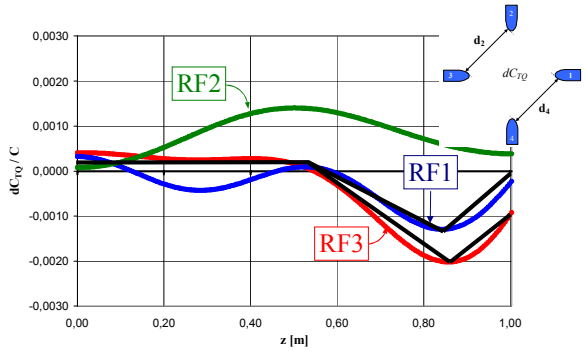

Fig. 8: $dC_{TQ}(z)$ evolution

On the contrary, the brazing has generated a S unbalance by a shortening of the relative distances in quadrant 1 vs quadrant 3. This mechanical contraction spans the section length.

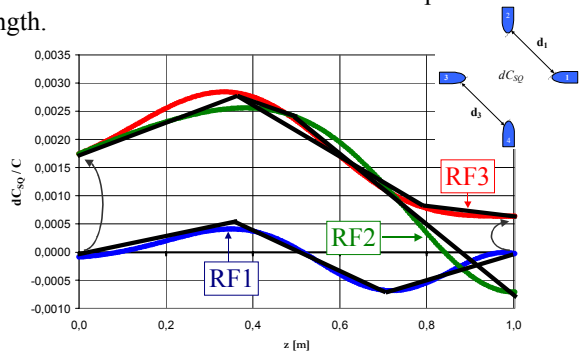

Fig. 9: $dC_{SQ}(z)$ evolution

6 CONCLUSION

The good correlation between RF diagnosis and mechanical probing has been verified. It permits to conclude from this RF estimation that the RFQ section mechanical symmetry is excellent.

The deduced capacitances for each quadrant are such that $|dC_i(z)|<10^{-2}$. Experimental tests made on our RFQ cold-model have shown that this equivalent mechanical default can be compensated with the slug tuners [5].

The brazing procedure has slightly modified one dipolar contribution but keeping its level very low.

The conditions of this RF diagnosis of individual RFQ sections are now optimised and this procedure is fully operational, requiring only a half-a-day test.

7 REFERENCES

[1] F. Simoens, A. France, J. Gaiffier, "A New RFQ Model Applied to the Estimation of Mechanical Defaults Distribution", this conference (EPAC 2002 Paris).

[2] F. Simoens & al., "A Fully Automated Test Bench for the Measurement of the Field Distribution in RFQ and Other Resonant Cavity", this conference.

[3] J. Gao, "The Precise Measurement of Electric and Magnetic Fields in a Resonant Cavity", pp 247-249, LINAC 1990

[4] P. Balleyguier, "Grille de pompage du RFQ", CEA internal report (26.06.2000).

[5] F. Simoens, A. France, J. Gaiffier, "A New RFQ Model applied to the Longitudinal Tuning of a Segmented, Inhomogeneous RFQ with Highly Irregularly Spaced Tuners", this conference.